Clinical and Laboratory Investigations

Dermatology

Dermatology 2004;208:21–26
DOI: 10.1159/000075041

Received: March 4, 2003
Accepted: July 2, 2003

Automated Extraction and Description of Dark Areas in Surface Microscopy Melanocytic Lesion Images

Giovanni Pellacani[a] Costantino Grana[b] Rita Cucchiara[b]
Stefania Seidenari[a]

Departments of [a]Dermatology and [b]Computer Engineering, University of Modena and Reggio Emila, Modena, Italy

Key Words
Melanoma · Epiluminescence · Dermoscopy · Image analysis · Computer-aided diagnosis · Videomicroscopy

Abstract
Background: Identification of dark areas inside a melanocytic lesion (ML) is of great importance for melanoma diagnosis, both during clinical examination and employing programs for automated image analysis. ***Objective:*** The aim of our study was to compare two different methods for the automated identification and description of dark areas in epiluminescence microscopy images of MLs and to evaluate their diagnostic capability. ***Methods:*** Two methods for the automated extraction of 'absolute' (ADAs) and 'relative' dark areas (RDAs) and a set of parameters for their description were developed and tested on 339 images of MLs acquired by means of a polarized-light videomicroscope. ***Results:*** Significant differences in dark area distribution between melanomas and nevi were observed employing both methods, permitting a good discrimination of MLs (diagnostic accuracy = 74.6 and 71.2% for ADAs and RDAs, respectively). ***Conclusions:*** Both methods for the automated identification of dark areas are useful for melanoma diagnosis and can be implemented in programs for image analysis.

Introduction

In contrast with common nevi, which generally show a homogeneous and regularly distributed pigmentation, brown to black pigment areas with irregular shape (the so-called blotches) or with an asymmetric distribution are frequently observable in melanomas [1–7].

Programs for image analysis enable the numerical description of some aspects of pigmented skin lesions, providing a reproducible quantification of several features and an aid for clinical diagnosis [8–21]. Different parameters, based on the measurement of brightness values, have been employed for the quantification of the overall darkness of the lesion. Great attention was paid to the automatic identification and the description of 'dark areas' inside the lesion employing the DBDermoMIPS system, but the method has not been clearly described [15, 17–19, 21]. Moreover, the concept of 'darkness' is not 'absolute', but it is related to human perception which can be influenced by the overall pigmentation of the lesion as well as by the color of the skin. In order to explore the influence of the evaluation of 'dark areas' in the diagnostic judgement of melanocytic lesions (MLs), we compared two methods for the identification of dark areas in videomicroscopic ML images. One enables the identification of 'absolute' dark areas (ADAs), whereas the other highlights 'relative' dark areas (RDAs) inside an ML. Some numerical descriptors of the aspect and distribution of the

KARGER

Fax + 41 61 306 12 34
E-Mail karger@karger.ch
www.karger.com

1018–8665/04/2081–0021$21.00/0

Accessible online at:
www.karger.com/drm

Stefania Seidenari
Department of Dermatology, University of Modena and Reggio Emilia
Largo dell Pozzo, 71
IT–41100 Modena (Italy)
Tel. +39 059 422 2464, Fax +39 059 422 4271, E-Mail seidenar@unimo.it

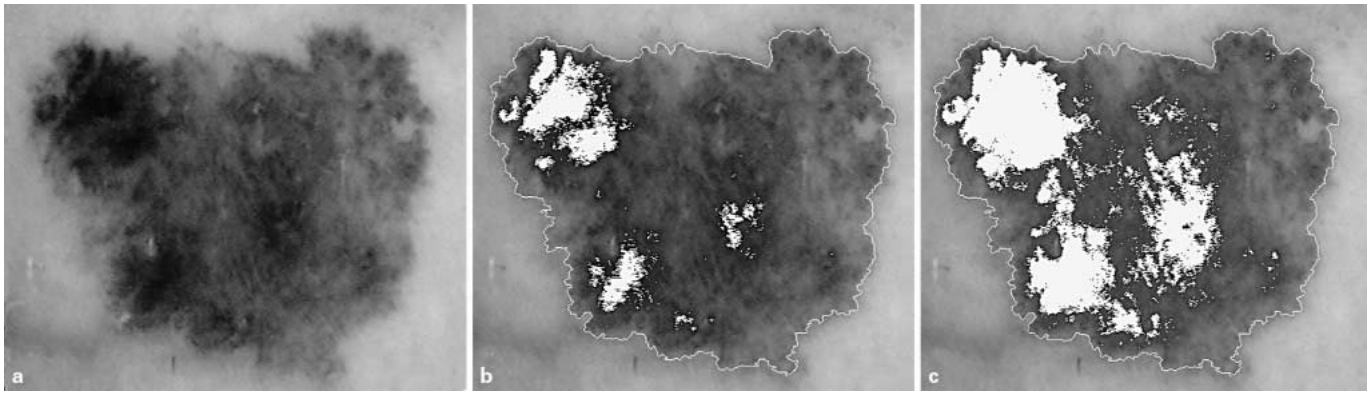

Fig. 1. Example of dark area identification in a melanoma: 20-fold videomicroscopic image (**a**); the same image with highlighted (in white) ADAs (**b**); the same image with highlighted (in white) RDAs (**c**).

identified areas were calculated. Subsequently, we tested the extracted features on a set of ML images to evaluate the influence of these descriptors in distinguishing between melanomas and nevi.

Material and Methods

Study Population and Instrument

339 images of pigmented skin lesions, referring to 113 melanomas and 226 melanocytic nevi, were studied. From a clinical point of view all lesions included in this study had been considered equivocal and were excised for histopathological examination. Prior to biopsy, images were acquired by means of a digital videomicroscope (VMS-110A, Scalar Mitsubishi, Tama-shi, Tokyo, Japan), with a 20-fold magnification enabling the whole lesion to be included in the monitor area. The instrument has been described elsewhere [15]. The images were digitized by means of a Matrox Orion frameboard and stored by an image acquisition program (VideoCap 8.09, DS-Medica, Milan, Italy), which runs under Microsoft Windows. The digitized images offer a spatial resolution of 768 × 576 pixels and a color resolution of 16 million colors.

Image Analysis Program

The image analysis program was created using MS visual C++ 6.0 both for dark area detection and description.

Dark Area Identification

Two different methods were employed for the selection of dark areas: the first permits the identification of ADAs, defined as areas which are darker than the skin. The second identifies the lesion area, the darkest with respect to the overall brightness of the lesion (RDAs). While the first method is based on absolute thresholds and may or may not identify a dark area, the second one will always find a dark area (fig. 1).

Absolute Dark Areas. Owing to the assumption that ADAs (fig. 1a) are darker than the skin, the mean brightness of the skin was first evaluated as a reference level. Subsequently, the ratio between the brightness of each lesion pixel and the skin's mean brightness was evaluated. If this value was lower than a given threshold, arbitrarily set at 0.130 on a visual basis, the pixel was considered 'dark'. In order to highlight peripheral dark areas which may have a clinical relevance in melanoma diagnosis, the threshold was linearly increased from 0.130 to 0.210 in a peripheral region consisting of all the lesion pixels exceeding 70% of the distance between the barycenter and the furthest border point in that direction (fig. 2).

Relative Dark Areas. The second approach is based on the algorithm for color reduction described by Heckbert [22], applied to the gray level image. In order to identify the darkest area inside the lesion (RDA; fig. 1c), the color histogram is divided into 4 zones following an iterative process that begins by dividing the gray level histogram along the median value and proceeds selecting the largest (as number of gray levels) of the two halves. The process is repeated until the number of required zones is obtained. The zone corresponding to the lowest gray levels is considered the RDA.

Parameter Calculation

A set of parameters is extracted both for ADAs and RDAs, in order to numerically describe the region properties. The first step consists in the detection of the lesion border [23] and the identification of reference geometrical measures (centroid and main inertia axes). Subsequently, the lesion is divided into 3 zones corresponding to different semantic parts. The *external zone* corresponds to the area within an arbitrarily selected distance of 15 pixels from the border, obtained employing the 4SSEDT algorithm by Danielsson [24]. The *internal zone* is formed by all the points with a ratio between the distance from the centroid and furthest border point in the same direction inferior to 0.5 (corresponding to 50% of the distance between the center and the border of the lesion). All other pixels belong to the *middle zone*. Each zone is then subdivided into 8 sectors formed by the division along the major and minor axes and along directions shifted 45° to the left and to the right of the axes.

Parameters, calculated for both types of 'dark areas' employed for lesion description and discrimination, are listed in table 1.

Statistics

For statistical analysis, the SPSS statistical package (release 10.0.06, 1999; SPSS Inc., Chicago, Ill., USA) was used. As basic statistics mean and standard deviation of the parameters obtained for

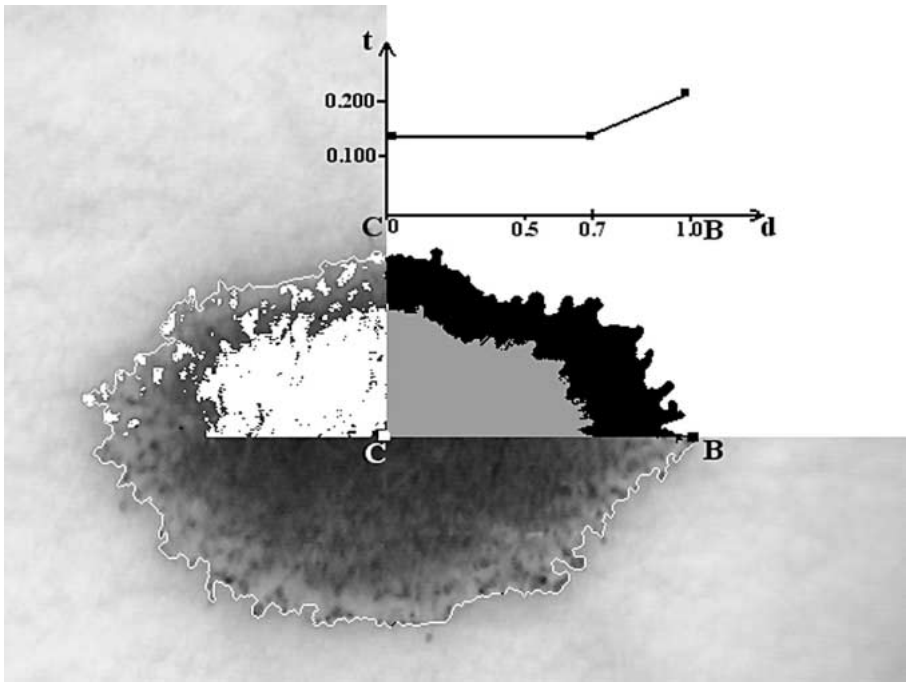

Fig. 2. ADA identification: the threshold is increased in the peripheral region, in order to identify peripheral dark areas. C = Centroid; B = border; d = relative distance from the centroid and the border; t = threshold.

Table 1. List of parameters and their clinical meaning

Parameter abbreviation	Range	Parameter description	Parameter meaning
Area	0–1	Number of pixels belonging to the region divided by the area of the lesion (proportion of the dark area with respect to the lesion area)	Dark area extension
DIST-BAR	0–1	Distance between the color region centroid and the lesion centroid, divided by the major axis length	Dark area distribution balance
SPRE	1–∞	It corresponds to the first invariant obtained from the sum of the second-order moments, with respect to the lesion centroid, divided by the squared area (mean of the square distance of the dark pixels from the barycenter); it describes the degree of compactness or sparseness of the region around the lesion centroid	Density of the dark area distribution
INT MID EXT	0–1	They correspond to the mean number of pixels per sector for each zone, describing the dark area involvement inside the internal (INT), middle (MID) and external (EXT) zones, respectively	Dark area distribution
REG-INT REG-MID REG-EXT	0–1	They correspond to the standard deviation of the number of pixels per sector for each zone, describing the regularity of dark area distribution inside the internal (INT), middle (MID) and external (EXT) zones, respectively	Regularity of the dark area distribution
SYM-MAX SYM-MIN	0–1	Three values, one for each zone, were first computed separately for major and minor axes as the absolute difference between the number of points located on each side; in order to obtain a single descriptor for each axis, the symmetry values of 3 zones were summed together and normalized by the region area; SYM-MAX and SYM-MIN represent the highest and lowest symmetry values along the major and minor axes thus extracted, respectively	Symmetry of the dark area distribution
Percent	0–100	Presence/absence	Percentage of lesions presenting the dark area

Table 2. Mean and standard deviation of the parameters calculated for ADAs and RDAs on 339 ML images comprising 113 melanomas and 226 melanocytic nevi

Parameters	ADA		RDA	
	MMs	nevi	MMs	nevi
Area	0.327 ± 0.261*	0.246 ± 0.224	0.262 ± 0.045	0.253 ± 0.023
DIST-BAR	0.101 ± 0.084*	0.057 ± 0.047	0.093 ± 0.057*	0.046 ± 0.028
SPRE	1.542 ± 3.257	1.060 ± 1.737	0.433 ± 0.174*	0.325 ± 0.106
INT	0.503 ± 0.354	0.497 ± 0.338	0.487 ± 0.186*	0.600 ± 0.139
REG-INT	0.151 ± 0.123	0.124 ± 0.087	0.233 ± 0.097*	0.179 ± 0.073
MID	0.342 ± 0.298*	0.248 ± 0.284	0.248 ± 0.081*	0.224 ± 0.073
REG-MID	0.176 ± 0.115*	0.099 ± 0.084	0.204 ± 0.081*	0.143 ± 0.055
EXT	0.084 ± 0.125*	0.034 ± 0.080	0.021 ± 0.036*	0.007 ± 0.011
REG-EXT	0.061 ± 0.066*	0.020 ± 0.032	0.027 ± 0.037*	0.008 ± 0.014
SYM-MAX	0.779 ± 0.204	0.819 ± 0.203	0.823 ± 0.119*	0.894 ± 0.064
SYM-MIN	0.565 ± 0.296*	0.667 ± 0.255	0.593 ± 0.218*	0.764 ± 0.129
Percent of presence	84.1*	65.5	100%	100%

* $p < 0.01$: statistically significant with respect to nevi. MMs = Malignant melanomas; for explanation of parameters, see table 1.

ADA and RDA were calculated for melanomas and nevi. Significant differences between nevus and melanoma values were evaluated using the Mann-Whitney U test for independent samples. A p value <0.01 was considered significant. In order to verify and to validate our methods for dark area description, the study population was randomly divided into a training set comprising 118 lesions (42 melanomas and 76 melanocytic nevi) and a test set comprising 221 lesions (71 melanomas and 150 melanocytic nevi). The values referring to parameters belonging to the training set underwent elaboration by means of multivariate discriminant analysis. Two separate equations were obtained, the first based on ADA values and the second on RDA values of the lesions belonging to the training set, and a threshold score for each equation was automatically established for the attribution of cases to groups. The same equation was applied to the test set. Moreover, the sum of the ADA and RDA scores was regarded as a global score for distinction between melanomas and nevi.

Receiver operating characteristic (ROC) analysis [25] was performed on the ADA, RDA and global score values in order to investigate sensitivity, specificity and diagnostic accuracy of the discriminant equations on ML classification. The area under the curve (AUC), which represents an index of the overall discriminant power, was calculated by the nonparametric trapezoidal method.

Results

Mean and standard deviation of parameters calculated for ADA and RDA are listed in table 2.

Absolute Dark Areas

ADAs were detected more frequently in melanomas compared with nevi (84.1 vs. 65.5%). In the former, ADAs were larger and more unevenly distributed, as shown by a greater distance from the barycenter and lower symmetry values. The central portion of the lesion was widely occupied by ADAs both in melanomas (50.3%) and in nevi (49.7%), whereas the intermediate and the external portions of the lesion were more extensively and nonhomogeneously covered by ADAs in melanomas (greater MID, REG-MID, OUT and REG-OUT values; for explanations, see table 1).

Discriminant analysis on ADA values identified DIST-BAR and REG-OUT as parameters useful for distinction between melanomas and nevi. The AUC value of ROC curves for ADAs was 0.813 for the training set and 0.734 for the test set, with an overall AUC of 0.763. For a score equal to 0, corresponding to the best diagnostic accuracy of 76.8%, a 69.0% sensitivity and a 84.5% specificity were obtained (table 3).

Relative Dark Areas

RDAs were more unevenly and irregularly distributed in melanomas with respect to nevi, as shown by greater DIST-BAR and SPRE values and lower symmetry ones. The central portion of the lesion was more widely occupied by RDAs in nevi, whereas the intermediate and the external portions of the lesion were more extensively and nonhomogeneously covered by RDAs in melanomas (greater MID, REG-MID, OUT and REG-OUT values).

Discriminant analysis on RDA values identified the Area, DIST-BAR, REG-INT and SYM-MIN as parame-

Table 3. Sensitivity, specificity and diagnostic accuracy for discriminant equation calculated for ADA, RDA and ADA + RDA scores on the training set (42 malignant melanomas and 76 nevi), the test set (71 malignant melanomas and 150 nevi) and the overall population (113 malignant melanomas and 226 nevi)

	Sensitivity %	Specificity %	Diagnostic accuracy, %
ADA			
Training set	71.4	86.8	79.1
Test set	67.6	83.3	75.5
Overall population	69.0	84.5	76.8
RDA			
Training set	61.9	90.8	76.3
Test set	56.3	86.6	71.5
Overall population	57.5	84.9	71.2
ADA + RDA			
Training set	85.7	80.3	83.0
Test set	70.4	78.0	74.2
Overall population	76.1	78.8	77.4

ters useful for distinction between melanomas and nevi. The AUC of ROC curves for RDA value was 0.832 for the training set and 0.742 for the test set, with an overall AUC of 0.773. For an RDA score equal to 0, corresponding to the best diagnostic accuracy of 71.2%, a 57.5% sensitivity and a 84.9% specificity were obtained (table 3).

Overall Score

Applying the ROC analysis to the overall score, obtained by the sum of ADA and RDA scores, an AUC of 0.826, a sensitivity of 76.1% and a specificity of 78.8%, with a diagnostic accuracy of 77.4%, were obtained (table 3).

Discussion

The identification of 'dark areas' inside MLs, as observed by means of surface microscopy tools, appears as a clue for the diagnosis of melanoma. In particular, the arrangement of the pigmentation seems to be relevant for distinguishing between benign and malignant lesions. In fact, a lesion with a dark area located in its center may arouse less clinical suspicion than a lesion with a similar dark but eccentrically placed or irregularly distributed pigmented blotch [3, 4]. Moreover, the asymmetric distribution of dark areas may influence the diagnostic judgement based on semiquantitative algorithms, such as the A parameter of the ABCD rule for dermoscopy [26] and the minor criterion 'presence of blotches' of the 7-point check list [27].

By means of image analysis programs, the darkness of the lesion is usually quantified by converting the color image into a luminance image in order to compute the histogram of the gray level image. The mean darkness of the lesion and its variance can be easily quantified, but these simple parameters do not enable a distinction between melanomas and nevi [8, 11]. Because melanomas are often variegated, the 'ratio of dark to light regions' [12], the 'variance of gray intensity' [16] and the 'color variegation', defined as the standard deviation of the lesion reflectance [14], have turned out to be characteristic parameters for melanoma diagnosis, but they only give information about the overall brightness of the lesion. The extension and the distribution of darkly pigmented structures, based on the calculation of polar moments of inertia, appeared useful for the distinction between melanomas and nevi, comprising Spitz/Reed nevi, too [15, 17–19, 21]. However, since the concept of 'dark area' is ambiguous and influenced by human perception, it is essential to define and describe the method of dark area identification employed for image analysis.

By means of our program we evaluated and compared two different procedures for the identification of dark areas. The first aimed at the identification of ADAs, corresponding to the darkly pigmented blotches, whereas the second enabled the highlighting of RDAs inside each lesion, regardless of the intensity of its pigmentation. ADAs were more frequently found in melanomas with respect to melanocytic nevi and were more unevenly and irregularly distributed, often involving the external zone. Employing the discriminant analysis, a good diagnostic accuracy was obtained (76.8%). On the other hand, the identification of RDAs appeared useful for the description of the symmetry of pigment distribution inside the lesion. In melanomas, these appeared more asymmetrically distributed and less aggregated with respect to melanocytic nevi. Their descriptors permitted the distinction between benign and malignant lesions with a diagnostic accuracy of 71.2%. Combining the two methods, an increase in the diagnostic performance was obtained, as shown by the greater AUC and the diagnostic accuracy of 77.4%. Our method represents a contribution to the refinement of programs for image analysis, based on the description of different lesion features, implemented with an automatic classifier. Computer diagnosis available for experts and for less experienced dermatologists, always

supported by clinical examination, may allow a wider diffusion of surface microscopic techniques and, consequently, an increase in diagnostic accuracy especially for thin melanomas.

Acknowledgment

This study was partially supported by a grant, No. 2001068929, from the Ministero dell'Istruzione dell'Università e della Ricerca.

References

1 Pehamberger H, Steiner A, Wolff K: In vivo epiluminescence microscopy of pigmented skin lesions. I. Pattern analysis of pigmented skin lesions. J Am Acad Dermatol 1987;17:571–583.

2 Kenet RO, Kang S, Kenet BJ, Fitzpatrick TB, Sober AJ, Barnhill RL: Clinical diagnosis of pigmented lesions using digital epiluminescence microscopy. Arch Dermatol 1993;129:157–174.

3 Steiner A, Binder M, Schemper M, Wolff K, Pehamberger H: Satistical evaluation of epiluminescence microscopy criteria for melanocytic pigmented skin lesions J Am Acad Dermatol 1993;29:581–588.

4 Nilles M, Boedeker RH, Schill WB: Surface microscopy of naevi and melanomas: Clues to melanoma. Br J Dermatol 1994;130:349–355.

5 Soyer HP, Smolle J, Leitinger G, Rieger E, Kerl H: Diagnostic reliability of dermoscopic criteria for detecting malignant melanoma. Dermatology 1995;190:25–30.

6 Menzies SW, Ingvar C, McCarthy WH: A sensitivity and specificity analysis of the surface microscopy features of invasive melanoma. Melanoma Res 1996;6:55–62.

7 Argenziano G, Soyer HP, Chimenti S, Talamini R, Corona R, Sera F, et al: Dermoscopy of pigmented skin lesions – Results of a consensus meeting via the internet. J Am Acad Dermatol 2003;48:679–693.

8 Cascinelli N, Ferrario M, Bufalino R, Zurrida S, Galimberti V, Mascheroni L, et al: Results obtained by using a computerized image analysis system designed as an aid to diagnosis of cutaneous melanoma. Melanoma Res 1992;2:163–170.

9 Schindewolf T, Stolz W, Albert R, Abmayr W, Harms H: Classification of melanocytic lesions with color and texture analysis using digital image processing. Anal Quant Cytol Histol 1993;15:1–11.

10 Green AC, Martin NG, Pfitzner J, O'Rourke M, Knight N: Computer image analysis in the diagnosis of melanoma. J Am Acad Dermatol 1994;31:958–964.

11 Hall PN, Claridge E, Morris Smith JD: Computer screening for early detection of melanoma – Is there a future? Br J Dermatol 1995;132:325–338.

12 Ganster H, Gelautz M, Pinz A, Binder M, Pehamberger H, Bammer M, Krocza J: Initial results of automated melanoma recognition; in Borgefors G (ed): Theory and Application of Image Analysis II: Selected Papers from the 9th SCIA, Scandinavian Conference on Image Analysis. Singapore, Word Scientific, 1995, pp 343–354.

13 Aitken JF, Pfitzner J, Battistutta D, O'Rourke PK, Green AC, Martin NG: Reliability of computer image analysis of pigmented skin lesions of Australian adolescents. Cancer 1996;78:252–257.

14 Gutkowicz-Krusin D, Elbaum M, Szwaykowski P, Kopf AW: Can early malignant melanoma be differentiated from atypical melanocytic nevus by in vivo techniques? II. Automatic machine vision classification. Skin Res Technol 1997;3:15–22.

15 Seidenari S, Pellacani G, Pepe P: Digital videomicroscopy improves diagnostic accuracy for melanoma. J Am Acad Dermatol 1998;39:175–181.

16 Binder M, Kittler H, Seeber A, Steiner A, Pehamberger H, Wolff K: Epiluminescence microscopy-based classification of pigmented skin lesions using computerized image analysis and an artificial neural network. Melanoma Res 1998;8:261–266.

17 Seidenari S, Pellacani G, Giannetti A: Digital videomicroscopy and image analysis with automatic classification for detection of thin melanomas. Melanoma Res 1999;9:163–171.

18 Andreassi L, Perotti R, Rubegni P, Burroni M, Cevenini G, Biagioli M, et al: Digital dermoscopy analysis for the differentiation of atypical nevi and early melanoma. Arch Dermatol 1999;135:1459–1465.

19 Pellacani G, Martini M, Seidenari S: Digital videomicroscopy with image analysis and automatic classification as an aid for diagnosis of Spitz nevus. Skin Res Technol 1999;5:266–272.

20 Ganster H, Pinz A, Rohrer R, Wildling E, Binder M, Kittler H: Automated Melanoma Recognition. IEEE Trans Med Imag 2001;20:233–239.

21 Rubegni P, Burroni M, Cevenini G, Perotti R, Dell'Eva G, Barbini P, et al: Digital dermoscopy analysis and artificial neural network for the differentiation of clinically atypical pigmented skin lesions: A retrospective study. J Invest Dermatol 2002;119:471–474.

22 Heckbert P: Color image quantization for frame buffer display. Comput Graphics (Proc SIGGRAPH '82) 1982;16:297–307

23 Grana C, Pellacani G, Cucchiara R, Seidenari S: A new algorithm for border description of polarized light surface microscopic images of pigmented skin lesions. IEEE Trans Med Imaging 2003;22:959–964.

24 Danielsson PE: Euclidean distance mapping. Comput Graphics Image Process 1980;14:227–248.

25 Hanley JA, McNeil BJ: The meaning and use of the area under a receiver operating characteristic (ROC) curve. Radiology 1982;143:29–36.

26 Nachbar F, Stolz W, Merkle T, Cognetta AB, Vogt T, Landthaler M, et al: The ABCD rule of dermatoscopy. J Am Acad Dermatol 1994;30:551–559.

27 Argenziano G, Fabbrocini G, Carli P, De Giorgi V, Sammarco E, Delfino M: Epiluminescence microscopy for the diagnosis of doubtful melanocytic skin lesions: Comparison of the ABCD rule of dermoscopy and a new 7-point checklist based on pattern analysis. Arch Dermatol 1998;134:1563–1570.